

https://dspace.org/

Effect of Turning Parameters on Cutting Forces Maximum Principal Stress and Maximum Interfacial Temperature on Medium Carbon AISI 1045 Steel Simulation and Comparative Studies

J Wambua; G Zoppi; W.L Woo; F Mwema; S Akinlabi ...

https://hdl.handle.net/10539/40535
SCOPUS

Downloaded from a DSpace repository. https://dspace.org/

Check for updates

RESEARCH ARTICLE

Macromolecular Symposia

www.ms-journal.de

Effect of Turning Parameters on Cutting Forces, Maximum Principal Stress, and Maximum Interfacial Temperature on Medium Carbon AISI 1045 Steel: Simulation and Comparative Studies

Job Wambua, Guillaume Zoppi, Wai-Lok Woo, Fredrick Mwema, Stephen Akinlabi, Michael Bodunrin, and Esther Akinlabi*

Medium carbon AISI 1045 steel is a hard to machine material attractive to the automotive and construction industries due to its high strength and excellent heat resistance. Finite element method (FEM) is used in this study to obtain the optimal parameters for turning AISI 1045 steel. The simulation data is obtained and analyzed using an L_{16} Taguchi orthogonal array (TOA). Three input parameters: cutting speed (*A*), depth of cut (*B*), and feed rate (*C*), and three responses: cutting forces (C_f), maximum interfacial temperature (T_{max}), and maximum principal stresses (σ_{max}) are considered and analyzed using analysis of variance (ANOVA). The optimal conditions obtained are 60 m min^{-1} for *A*, 0.3 mm for *B*, and 0.4 mm rev^{-1} for *C*. The depth of cut and feed rate contribute the largest to the C_f (80.98%) and T_{max} (38.56%), respectively. All the parameters contribute approximately equal toward the σ_{max}. Comparison between the FEM values and literature experimental data shows that FEM can be used to predict optimal turning parameters with differences of ≈5%. This study gives a reference prediction model for the optimal machining parameters of medium carbon AISI 1045 steel and other related materials, which can be used, alongside experiments, to reduce the overall machining costs.

1. Introduction

The machining industry is interested in reducing production costs incurred from trial and error choosing of machining conditions for various materials.[1] As such, numerical simulations combined with statistical optimization models are very useful to visualize the machining process and reduce experimental trials. In this study, a finite element method (FEM) is used to simulate the turning process of medium carbon AISI 1045 steel. The material has been widely used in the automotive and construction industries due to its high mechanical strength and excellent heat resistance.[2] In these applications, the material requires machining where high cutting forces, stresses, and localized temperatures are often experienced from shear deformation and frictional forces generated by the movement and flow of chips,[3] which lead to tool and machined surface degradation, and as such the material is said to be hard-to-machine. These machining responses are often affected by the machining parameters such as cutting speed, feed rate, and depth of cut.

Various studies have been conducted to evaluate the parameter–response interactions. For instance, it was reported that an increase in cutting speeds results to tool damage during the turning of medium carbon steel.[4] In another study by Kara et al.[5] it was noted that the cutting parameters affected the cutting forces, cutting temperatures, and rate of tool wear in milling of 17-4 PH stainless steel. The optimal outputs were observed at the least cutting speed (70 m min^{-1}) and feed rate (0.06 mm per tooth). Akgün et al.[6] also studied the turning of AISI H13 steel using coated tools and the resulting cutting forces, surface roughness, cutting temperature, and power consumption. Other authors have reported the main turning parameters affecting machined components.[3,7]

The current focus has been on the optimization of the major responses, such as surface roughness, cutting forces, and material removal rate. As such, there is a gap in the optimization of interfacial temperature and principal stresses generated. Therefore, this study, for the first time, utilizes finite element modeling to conduct a multi-response evaluation of C_f, T_{max}, and σ_{max} generated and their interaction with the turning parameters of

J. Wambua, G. Zoppi, W.-L. Woo, F. Mwema, S. Akinlabi, E. Akinlabi
Faculty of Engineering and Environment
Northumbria University
Ellison Place, Newcastle upon Tyne NE1 8ST, UK
E-mail: job.wambua@northumbria.ac.uk

F. Mwema
Department of Mechanical Engineering Science
University of Johannesburg
Johannesburg 2006 South Africa

M. Bodunrin
School of Chemical and Metallurgical Engineering, DSI-NRF Centre of Excellence in Strong Materials
University of the Witwatersrand
Johannesburg 2050 South Africa

The ORCID identification number(s) for the author(s) of this article can be found under https://doi.org/10.1002/masy.202300189

DOI: 10.1002/masy.202300189

 © 2024 Wiley-VCH GmbH

Table 1. Turning simulation model conditions.

Input parameters	Value
Tool, toolholder geometry and tool temperature	D shape, MVUNR, and 30 [°C]
Tool-environment convection coefficient	0.02 [NS^{-1} mm^{-1} °C]
Workpiece and environmental temperature	30 [°C] and 30 [°C]
Workpiece diameter and angle cut	50 [mm] and 15°
Number of elements, workpiece: cutting tool	30 000:20 000
Heat transfer coefficient and friction factor	45 [NS^{-1} mm^{-1} °C] and 0.6
Workpiece: tool movement	Constrained in all directions: y-direction

medium carbon AISI 1045 steel. The experimental data from literature was used to validate the FEM model.[3,8]

2. Materials and Simulation Modeling

Medium carbon AISI 1045 steel was selected from the DEFORM 3D software database (Elastic modulus = 200 GPa, Poisson's ratio of 0.290, Brinell hardness of 200, and ultimate tensile strength = 565 MPa) and tungsten carbide as the cutting tool. The workpiece and the cutting tool were modeled as plastic and rigid objects, respectively. The finite element model was developed through the Lagrangian incremental model for continuous remeshing with material removal. The boundary conditions adopted are shown in **Table 1**. The tool and workpiece, as designed in the software, and an example of the FEM interface for the T_{max} are shown in **Figure 1**a and b, respectively.

The design of experiments was done using Taguchi's approach in MINITAB 21 with three factors as shown in **Table 2**.

Using an L_{16} TOA displayed in **Table 3**, simulation studies were conducted to obtain and analyze the results using signal-to-noise ratios (S/NRs). The *Smaller-is-the-better* model was chosen to optimize the responses (toward zero).[9] Then, an analysis of variance (ANOVA) was conducted to study the contribution of the parameters to machinability.

Table 2. Turning parameters for the simulation model.

Parameters	Symbol	Level			
		1	2	3	4
Cutting speed [m min^{-1}]	*A*	60	90	120	170
Depth of cut [mm]	*B*	0.3	0.4	0.5	0.7
Feed rate [mm rev^{-1}]	*C*	0.3	0.4	0.5	0.7

3. Results and Discussion

The highest S/NR values for each response were used to obtain the optimal turning parameters. These optimal parameters (displayed in **Figure 2**) are a combination of $A_2B_1C_1$ for the C_f, $A_3B_2C_3$ for the σ_{max}, and $A_1B_1C_2$ for the T_{max}.

3.1. Analysis of Variance

A confidence level of 95% was utilized in the ANOVA to determine the significance level, percentage contribution, and *p*-values of each parameter in relation to the responses. The % contribution was computed from the ratio of the adjusted mean squares (Adj MS) to the total of the mean of squares. The Adj MS were also used by the Minitab software to compute the *F*- and *p*-values to show the level of significance of the parameters toward the responses. These findings are shown in **Table 4**.

The depth of cut had the highest contribution to the C_f (80.98%) and σ_{max} (26.02%), while the cutting speed had the lowest (1.38% and 22.50%, respectively). However, the cutting speed had the highest significance toward the C_f (a small change in cutting speed translated to a huge change in the C_f). The other parameters had low significance toward the responses. The feed rate had the highest contribution toward the T_{max} (38.56%) while the cutting speed had the lowest (12.06%). These trends could be linked to various explanations in literature.[4,5]

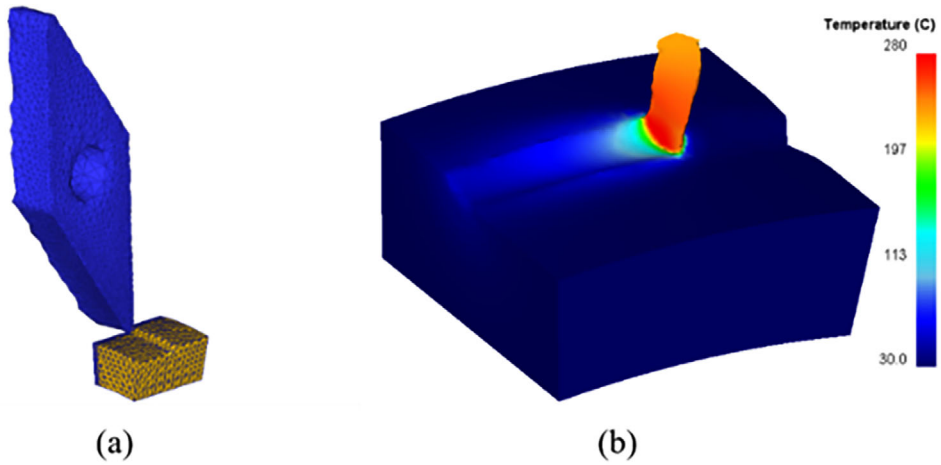

Figure 1. a) The meshed tool and workpiece, b) sample finite element method (FEM) interface for the T_{max}.

© 2024 Wiley-VCH GmbH

15213900, 2024, 3, Downloaded from https://onlinelibrary.wiley.com/doi/10.1002/masy.202300189 by South African Medical Research, Wiley Online Library on [24/07/2024]. See the Terms and Conditions (https://onlinelibrary.wiley.com/terms-and-conditions) on Wiley Online Library for rules of use; OA articles are governed by the applicable Creative Commons License

Table 3. L_{16} Taguchi orthogonal array with corresponding output parameters and signal-to-noise ratios (S/NRs).

Exp no.	A [m min^{-1}]	B [mm]	C [mm rev^{-1}]	C_f [N]	C_f (S/NRs)	σ_{max} [MPa]	σ_{max} (S/NRs)	T_{max} [°C]	T_{max} (S/NRs)
1	60	0.3	0.3	277.145	−48.85	3380	−70.58	290	−49.25
2	60	0.4	0.4	494.515	−53.88	3360	−70.53	318	−50.05
3	60	0.5	0.5	923.392	−59.31	3550	−71.00	672	−56.55
4	60	0.7	0.7	1528.305	−63.68	3300	−70.37	459	−53.24
5	90	0.3	0.4	323.202	−50.19	3510	−70.91	343	−50.71
6	90	0.4	0.3	366.128	−51.27	3620	−71.17	995	−59.96
7	90	0.5	0.7	1067.723	−60.57	3140	−69.94	406	−52.17
8	90	0.7	0.5	1228.027	−61.78	3260	−70.26	514	−54.22
9	120	0.3	0.5	386.198	−51.74	3390	−70.60	433	−52.73
10	120	0.4	0.7	675.908	−56.60	3210	−70.13	452	−53.10
11	120	0.5	0.3	561.761	−54.99	3180	−70.05	909	−59.17
12	120	0.7	0.4	1118.862	−60.98	3630	−71.20	576	−55.21
13	170	0.3	0.7	484.976	−53.71	3810	−71.62	482	−53.66
14	170	0.4	0.5	532.539	−54.53	2570	−68.20	470	−53.44
15	170	0.5	0.4	1041.138	−60.35	2960	−69.43	545	−54.73
16	170	0.7	0.3	918.642	−59.26	9800	−85.93	638	−56.10

3.2. Optimal Parameters Confirmatory Test Using FEM

The confirmatory test conducted on the combined optimal conditions depicted that the best conditions occur at $A_1 = 60$ m min^{-1}, $B_1 = 3$ mm, and $C_2 = 0.4$ mm rev^{-1}. This is displayed in **Figure 3**. The combination $A_2B_1C_1$ spiked at around 2300 N and 22 000 MPa owing to built-up edges on the tool leading to generation of high cutting forces and stresses.[10]

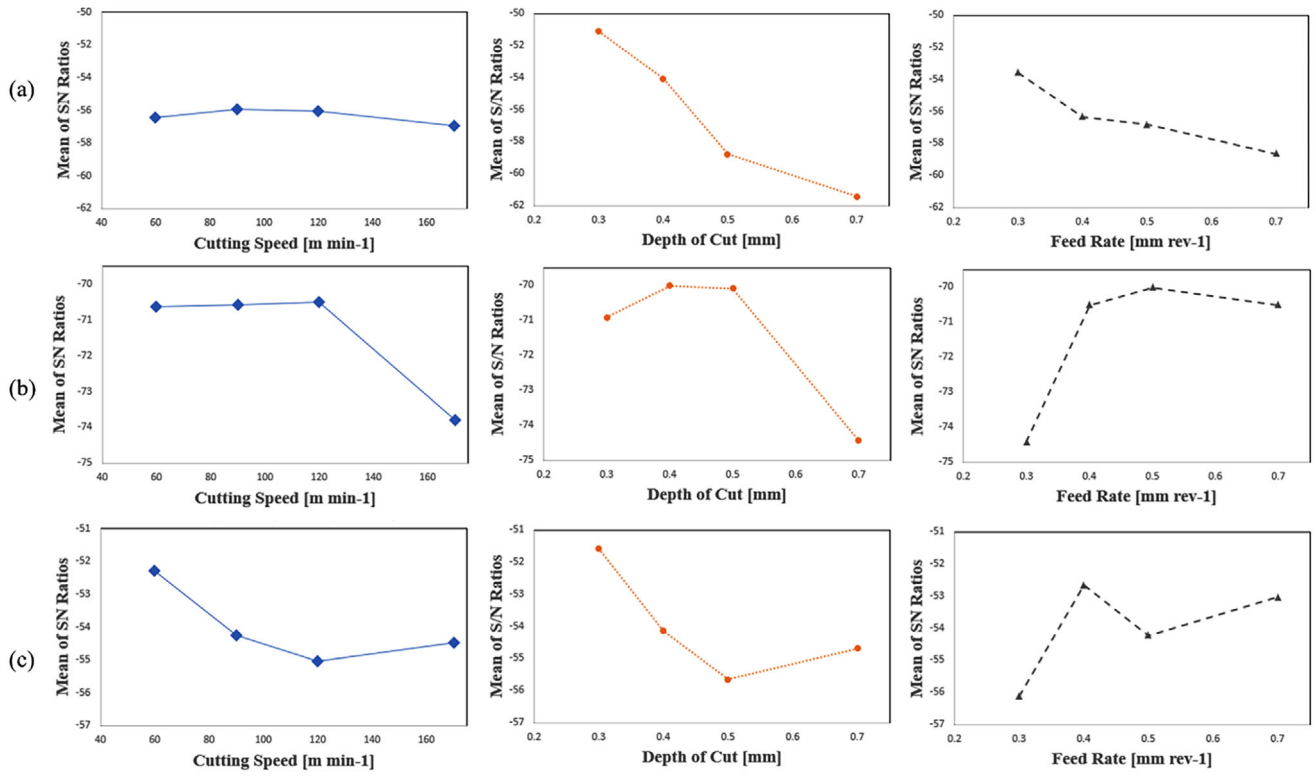

Figure 2. Main effects plots for the signal-to-noise ratios (S/NRs) of a) C_f, b) σ_{max}, and c) T_{max}.

© 2024 Wiley-VCH GmbH

15213900, 2024, 3, Downloaded from https://onlinelibrary.wiley.com/doi/10.1002/masy.202300189 by South African Medical Research, Wiley Online Library on [24/07/2024]. See the Terms and Conditions (https://onlinelibrary.wiley.com/terms-and-conditions) on Wiley Online Library for rules of use; OA articles are governed by the applicable Creative Commons License

Table 4. Results of the ANOVA.

Source	Adj MS	% Contribution	*F*-value	*p*-value	Significance
Cutting force					
Cutting speed	9628	1.38	0.89	0.5000	Low
Depth of cut	564 355	80.98	51.93	0.0001	High
Feed rate	112 083	16.08	10.31	0.0090	High
Error	10 867	1.56			
Maximum principal stress					
Cutting speed	15 269 956	22.50	0.88	0.5030	Low
Depth of cut	17 656 456	26.02	1.02	0.4490	Low
Feed rate	17 561 606	25.88	1.01	0.4510	Low
Error	17 382 156	25.61			
Maximum interfacial temperature					
Cutting speed	18 901	12.06	0.55	0.6680	Low
Depth of cut	42 877	27.36	1.24	0.3740	Low
Feed rate	60 422	38.56	1.75	0.2560	Low
Error	34 498	22.02			

Adj MS, adjusted mean squares; ANOVA, analysis of variance.

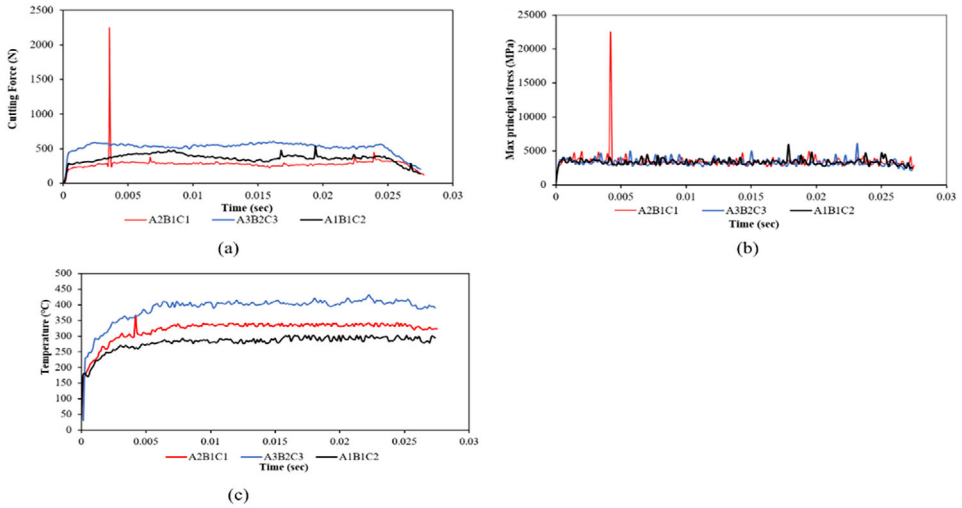

Figure 3. Variation of a) C_f, b) σ_{max}, and c) T_{max} in finite element method (FEM) analysis with optimized conditions.

Table 5. Sample comparison between experimental and finite element method (FEM) values.

Response	Turning parameter symbol	FEM value	Experimental value	FEM (average)	Experimental value (average)	% Difference
C_f [N]	*A* [m min^{-1}]	90	94.2	250 N	260 N [8]	3.92%
	B [mm]	0.3	1.0			
	C [mm rev^{-1}]	0.3	0.191			
σ_{max} [MPa]	*A* [m min^{-1}]	120	–	3100 MPa	–	–
	B [mm]	0.4	–			
	C [mm rev^{-1}]	0.5	–			
T_{max} [°C]	*A* [m min^{-1}]	60	70	260 °C	247 °C[3]	5.13%
	B [mm]	0.3	1.0			
	C [mm rev^{-1}]	0.4	0.246			

© 2024 Wiley-VCH GmbH

15213900, 2024, 3, Downloaded from https://onlinelibrary.wiley.com/doi/10.1002/masy.202300189 by South African Medical Research, Wiley Online Library on [24/07/2024]. See the Terms and Conditions (https://onlinelibrary.wiley.com/terms-and-conditions) on Wiley Online Library for rules of use; OA articles are governed by the applicable Creative Commons License

3.3. Comparison of FEM Optimal Parameters with Experimental Data

The FEM results were compared with related experimental studies (**Table 5**).[3,8] An approximate percentage difference of about 5% was observed in the results.

4. Conclusion

From the study, the optimal parameters for the C_f, σ_{max}, and T_{max} are 60 m min^{-1} (*A*), 0.3 mm (*B*), and 0.4 mm rev^{-1} (*C*). The depth of cut affects the C_f (80.98%) the most. An increase in the machining parameters increases the thermal deformation regions, leading to high machining stresses. The feed rate contributes the largest toward the T_{max} (38.56%) owing to high deformation energy and friction coefficient at the tool-workpiece interface. Comparisons of the FEM and experiments show that FE simulation can predict optimal turning parameters and their impacts on machined components.

Acknowledgements

The authors acknowledge the University of the Witwatersrand for the DEFORM 3D license.

Conflict of Interest

The authors declare no conflicts of interest.

Data Availability Statement

Data related to this article can be provided upon request.

Keywords

cutting force, finite element method, maximum interfacial temperature, maximum principal stress, Taguchi's technique

Received: October 17, 2023
Revised: February 6, 2024

[1] J. Outeiro, W. Cheng, F. Chinesta, A. Ammar, *J. Manuf. Mater. Process.* **2022**, *6*, 3.
[2] R. Karimbaev, S. Choi, Y. S. Pyun, A. Amanov, *Materials (Basel)* **2020**, *13*, 859.
[3] B. Guimarães, J. Rosas, C. M. Fernandes, D. Figueiredo, H. Lopes, O. C. Paiva, F. S. Silva, G. Miranda, *J. Manuf. Mater. Process.* **2023**, *7*, 1.
[4] K. Jarosz, P. Niesłony, P. Löschner, *Arch. Mech. Technol. Mater.* **2018**, *38*, 1.
[5] F. Kara, N. Bulan, M. Akgün, U. Köklü, *Eng. Sci.* **2023**, *26*, 961.
[6] M. Akgün, B. Özlü, F. Kara, *J. Mater. Eng. Perform.* **2023**, *32*, 1390.
[7] V. P. Wani, H. A. Chavan, R. J. Pawar, *Mater. Today Proc.* **2023**, *2*, 232.
[8] B. D. Jerold, M. P. Kumar, *J. Manuf. Process.* **2011**, *13*, 2.
[9] J. M. Wambua, F. M. Mwema, B. Tanya, T. C. Jen, *Int. J. Manuf. Mater. Mech. Eng.* **2022**, *12*, 1.
[10] V. Sivaraman, S. Sankaran, L. Vijayaraghavan, *Proc. CIRP* **2012**, *4*, 157.

© 2024 Wiley-VCH GmbH

15213900, 2024, 3, Downloaded from https://onlinelibrary.wiley.com/doi/10.1002/masy.202300189 by South African Medical Research, Wiley Online Library on [24/07/2024]. See the Terms and Conditions (https://onlinelibrary.wiley.com/terms-and-conditions) on Wiley Online Library for rules of use; OA articles are governed by the applicable Creative Commons License